

RSC Advances



This is an *Accepted Manuscript*, which has been through the Royal Society of Chemistry peer review process and has been accepted for publication.

Accepted Manuscripts are published online shortly after acceptance, before technical editing, formatting and proof reading. Using this free service, authors can make their results available to the community, in citable form, before we publish the edited article. This *Accepted Manuscript* will be replaced by the edited, formatted and paginated article as soon as this is available.

You can find more information about *Accepted Manuscripts* in the [Information for Authors](#).

Please note that technical editing may introduce minor changes to the text and/or graphics, which may alter content. The journal's standard [Terms & Conditions](#) and the [Ethical guidelines](#) still apply. In no event shall the Royal Society of Chemistry be held responsible for any errors or omissions in this *Accepted Manuscript* or any consequences arising from the use of any information it contains.

Influence of anionic co-ligands on the structural diversity and catecholase activity of copper(II) complexes with 2-methoxy-6-(8-iminoquinolinylmethyl)phenol

Milan Shyamal,^a Tarun Kanti Mandal,^b Anangamohan Panja*^c and Amrita Saha*^a

^a Department of Chemistry, Jadavpur University, Kolkata 700 032, India

^b Department of Biotechnology, Haldia Institute of Technology, Hatiberia, Haldia, West Bengal 721 657, India

^c Postgraduate Department of Chemistry, Panskura Banamali College, Panskura RS, Purba Medinipur, West Bengal 721 152, India

Corresponding Author

E-mail: ampanja@yahoo.co.in (A. P.); amritasahachemju@gmail.com (A. S.)

ABSTRACT

A novel dinuclear copper(II) complex, $[\text{Cu}_2\text{L}_2(\mu_{1,1}\text{-N}_3)_2]$ (**1**), and a mononuclear copper(II) complex, $[\text{CuL}(\text{NCO})]$ (**2**), have been synthesized from a planar tridentate ligand 2-methoxy-6-(8-iminoquinolinylmethyl)phenol (HL) together with pseudohalides as coligands, and the solid state structures were determined by the X-ray crystallography. Structural characterizations reveal that the geometry of centrosymmetrically related copper(II) centers in **1** is square pyramidal while it is square planar in **2**. The impact of the structural diversity was found on their catechol oxidase mimicking activity. Strongly bridging azide ions being substitutionally inert complex **1** is inactive towards the

catecholase activity, while mononuclear analogue **2** exhibits moderately strong catechol oxidase activity. The ESI-MS positive spectrum of a mixture of complex **2** and 3,5-DTBC₂ shows a peak corresponding to both superoxo and substrate bound species, Na[CuL(O₂)(3,5-DTBC₂)]⁺, suggesting that both the dioxygen and substrate simultaneously coordinated to metal center at the catalytic cycle. Most importantly, complex **2** not only represents the mononuclear class of copper(II) compounds that rarely visited for the study of catecholase mimicking activity but also the first example of a mononuclear square planar complex exhibiting catechol oxidase activity.

Introduction

Dioxygen represents the ultimate in “green” oxidants as it is atom economic and freely available in the environment. Metalloenzymes that activate molecular dioxygen are of great interest because they facilitate spin forbidden interaction between molecular dioxygen and organic substances.¹⁻³ The study of model complexes of such enzymes not only helps to understand the biochemical phenomena in the natural systems but also provides clue to the development of small molecule catalysts for specific oxidation reactions under mild conditions.⁴⁻⁶ Therefore, most of the focus of ongoing biomimetic and bioinspired chemistry is to the synthesis and reactivity studies of transition metal-based model complexes for metalloenzymes that show oxidase or oxygenase activity.^{7,8}

One of the major enzymes that utilizes molecular dioxygen is catechol oxidase, a lesser explored member of the type-III copper proteins.⁹ This enzyme belongs to the class of polyphenol oxidases that catalyzes exclusively the oxidation of a wide range of *o*-diphenols (catechols) to the corresponding *o*-quinones in a process known as catecholase activity.¹⁰⁻¹² Quinones are highly reactive compounds which undergo auto polymerization to produce melanin, a brown colored pigment, and this process is most likely responsible for protecting

damaged tissues against pathogens and insects.¹³ The structural determination of the catechol oxidase has encouraged an extensive investigation of model compounds to understand the structure–property relationship.^{9, 14–18} As the active site of the structure consists of a dicopper(II) moiety, several dinuclear copper(II) complexes derived from N/O donor dinucleating ligands have been mainly employed for this purpose.^{9, 14–30} In addition to the dicopper(II) systems, a few mononuclear copper(II) complexes^{31–35} and even a few copper(II) clusters and polymers have been found as active catalysts.³⁶ Although few structure-property correlations have been performed, they do not cover a wide range of compounds but only applicable for a set of limited compounds. All these facts indicate that exploration of the possibility of exhibiting catecholase activity by new types of compounds in terms of any of the following deserves importance: metal–metal distance, flexibility of the ligand, type of exogenous ligand and coordination geometry around the metal ion.

We have recently reported several transition metal complexes those were found to be efficient functional models for phenoxazinone synthase^{37–40} and catechol oxidase.⁴¹ Close inspection of our previous results suggests that both the substitutionally labile coordination sites and the electronic environment of the metal center play important role for the biomimetic catalytic activity.^{37–41} From the reports in the literature on various copper(II) model compounds^{14–30} and from the crystal structure of catechol oxidase,⁹ it is also clear that the active site of functional models must have free coordination sites available for substrate binding. Therefore, the ligands having lesser number of donor atoms are more promising. As a part of our ongoing study in the development of functional model complexes of various oxidase metalloenzymes,^{37–41} we report herein the synthesis and crystal structures of a new dinuclear copper(II) complex, $[\text{Cu}_2\text{L}_2(\mu_{1,1}\text{-N}_3)_2]$ (**1**), and a mononuclear copper(II) complex, $[\text{CuL}(\text{NCO})]$ (**2**), derived from a tridentate Schiff-base ligand, 2-methoxy-6-(8-iminoquinolinylmethyl)phenol (HL) (Scheme 1) together with

exogenous pseudohalide coligands (N_3^- and NCO^- , respectively). Role of the exogenous pseudohalide coligands on the structural diversity and on the relative catecholase activity of the complexes have also been explored.

Experimental section

Materials and physical measurements

All reagent or analytical grade chemicals and solvents were purchased from commercial sources and used as received. Elemental analyses for C, H and N were carried out using a Perkin-Elmer 240 elemental analyzer. Infrared spectra ($400\text{--}4000\text{ cm}^{-1}$) were recorded from KBr pellets on a Nicolet Magna IR 750 series-II FTIR spectrophotometer. Absorption spectra were measured using a Shimadzu UV-2450 spectrophotometer with a 1 cm path-length quartz-cell. Electrochemical data were collected on an EG & G Princeton Applied Research potentiostat model 263A with a Pt working electrode, Pt auxiliary electrode and Ag/AgCl reference electrode. Electrospray ionization (ESI-MS positive) mass spectrometric studies were performed using Micromass Q-tof-Micro Quadruple and Q-tof-Micro YA263 mass spectrophotometers.

Synthesis of Schiff base ligand HL

The tridentate Schiff base ligand (HL) was prepared by the standard method.⁴² Briefly, 1.0 mmol of 8-aminoquinoline (145 mg) were mixed with 1.0 mmol of *o*-vanillin (152 mg) in 20 mL of methanol. The resulting solutions were heated to reflux for ca. 1 h, and allowed to cool. The dark orange methanol solution was used directly for complex formation.

Synthesis of complex $[\text{Cu}_2\text{L}_2(\mu_{1,1}\text{-N}_3)_2]$ (1)

A 20 mL methanol solution of HL (1.0 mmol) was combined with a solution of

$\text{Cu}(\text{OAc})_2 \cdot \text{H}_2\text{O}$ (202 mg, 1.0 mmol) and another 5 mL aqueous solution of sodium azide (65 mg, 1.0 mmol). The resulting mixture was heated to reflux for 1 h during which time color of the solution changed to dark brown. The reaction mixture was then filtered and kept at room temperature. Analytically pure dark-brown crystals suitable for X-ray diffraction were obtained from the solution after several days, which was collected by filtration and washed with methanol/ether and air dried. Yield: 272 mg (71 %). Anal. Calcd. for $\text{C}_{34}\text{H}_{26}\text{N}_{10}\text{O}_4\text{Cu}_2$: C 53.33%, H 3.42%, N 18.29 %. Found: C 53.54%, H 3.35%, N 17.96 %. IR (cm^{-1} , KBr): 3041w, 2925w, 2046vs, 1603m, 1539w, 1504w, 1429s, 1404w, 1334w, 1245m, 1215s, 1174m, 1090w, 980w, 831w, 765w, 734m, 671w. UV-Vis $\lambda_{\text{max}}/\text{nm}$ ($\epsilon/\text{dm}^3\text{mol}^{-1}\text{cm}^{-1}$) in DMF/methanol: 353 (19975), 462 (9986), 615 (92).

Synthesis of complex $[\text{CuL}(\text{NCO})]$ (**2**)

Complex **2** was synthesized following the very similar procedure as described for complex **1** except that sodium cyanate was used instead of sodium azide. Color: Dark brown, Yield: 306 mg (80%). Anal. Calcd. for $\text{C}_{18}\text{H}_{13}\text{N}_3\text{O}_3\text{Cu}$: C 56.47%, H 3.51%, N 10.97 %. Found: C 56.56%, H 3.65%, N 10.72 %. IR (cm^{-1} , KBr): 3056w, 2960w, 2835w; 2204vs, 1608vs, 1602w, 1553w, 1508w, 1460s, 1414w, 1401w, 1290s, 1249s, 1240s, 1101m, 1005m, 982w, 855w, 758w, 744m, 684w. UV-Vis $\lambda_{\text{max}}/\text{nm}$ ($\epsilon/\text{dm}^3\text{mol}^{-1}\text{cm}^{-1}$) in DMF/methanol: 351 (11890), 456 (5520), 627 (121).

X-ray crystallography

Single crystal X-ray data of complexes **1** and **2** were collected on a Bruker SMART APEX-II CCD diffractometer using graphite monochromated Mo $\text{K}\alpha$ radiation ($\lambda = 0.71073 \text{ \AA}$) at room temperature. Data processing, structure solution, and refinement were performed using Bruker Apex-II suite program. All available reflections to $2\theta_{\text{max}}$ were

harvested and corrected for Lorentz and polarization factors with Bruker SAINT plus.⁴³ Absorption corrections, inter-frame scaling, and other systematic errors were performed with SADABS.⁴³ The structures were solved by the direct methods and refined by means of full matrix least-square technique based on F^2 with SHELX-97 software package.⁴⁴ All the nonhydrogen atoms were refined with anisotropic thermal parameters. All the hydrogen atoms belonging to carbon were placed in their geometrically idealized positions, and all of them were constrained to ride on their parent atoms. Crystal data and details of data collection and refinement for **1** and **2** are summarized in Table 1.

Computational method

All the theoretical calculations were carried out by DFT method implemented in Gaussian 09 software.⁴⁵ Ground states of the ligand and complex **2** were optimized by DFT method with B3LYP exchange correlation functional in methanol (MeOH) media associated with PCM model (Table S1). The absorption spectra in methanol were calculated by time dependent density functional theory (TDDFT) method, while for the complex split basis set was used. The 6-31g (d) basis set was used for H, C, N and O atoms and LANL2DZ was used for Cu atom (Table S1). For all the intermediates and transition state UB3LYP functional was used for mechanistic interpretation (Table S1). The frontier molecular orbitals were prepared by using GaussView 5.0 software package and the molecular orbital contribution from groups or atoms was calculated by GaussSum 3.0 program.

Catalytic oxidation of 3,5-DTBCH₂

The catecholase activity of the complexes was studied by the reaction of 200 equivalents of 3,5-di-*tert*-butylcatechol (3,5-DTBCH₂) with 2×10^{-5} M solutions of the complexes under aerobic conditions at 25 °C in methanol/DMF (50:1 v/v). The reaction was

followed spectrophotometrically by monitoring increase in the absorbance as a function of time at ca. 400 nm which is characteristic of *o*-quinone formation. To determine the dependence of rate of the reaction on substrate concentration and various kinetic parameters, 2×10^{-5} M solutions of the complexes were treated with at least 10 equivalents of substrate to follow pseudo-first order condition. To check the rate dependency on catalyst concentrations similar set of experiments were performed at fixed concentration of substrate with various catalyst concentrations. The initial rate method was applied to determine the rate of a reaction, and the average initial rate over three independent measurements was recorded.

Results and discussion

Syntheses and general characterizations

The synthetic route employed for the preparation of complexes **1** and **2** is depicted in Scheme 1. The tridentate ligand (HL) was synthesized by the Schiff base condensation of equimolecular mixture of *o*-vanillin and 8-aminoquinoline in methanol under reflux. Reaction of $\text{Cu}(\text{OAc})_2 \cdot \text{H}_2\text{O}$, Schiff base ligand (HL), and a coligand (azide ion) in 1:1:2 molar ratio in methanol/water medium afforded **1** in high yield. Very similar procedure but using sodium cyanate instead of azide as a coligand produced only **2**. The nature of the solid crystalline products was examined for both the compounds, and no visible difference in the crystalline state was observed, indicating that the solids are not mixtures of different compounds. The results of elemental analyses also confirm that the compositions of the complexes are eventually same as those obtained from X-ray diffractions.

Both the compounds were characterized by the FT-IR spectroscopy and important infrared bands of them are given in the experimental section. The IR spectra of these complexes are very similar to each other with regards to mono-anionic tridentate L ligand.

IR spectra show strong and sharp bands for $\nu(\text{C}=\text{N})$ at 1603 and 1608 cm^{-1} for complexes **1** and **2**, respectively, indicating the presence of Schiff base ligand. In the spectrum of complex **2**, a strong band at 2204 cm^{-1} is attributed to the presence of N-coordinated cyanate group. Whereas the IR spectrum shows only a single sharp absorption band in **1**, consistent with the presence of only one type of azide (bridging azide) in the structure and it appears at lower frequency, 2046 cm^{-1} , which is in agreement with the asymmetric bridging.⁴⁶⁻⁵¹ Both the complexes are electrochemically active which is the signature of the transition metal complexes. The cyclic voltammograms of the complexes show an electrochemically irreversible peak at -0.80 V and -0.66 V for complexes **1** and **2**, respectively, which are assigned to the reduction from copper(II) to copper(I) centers

UV-vis spectroscopy and DFT study

Both the complexes are practically insoluble in acetonitrile and partly soluble in methanol, while they are sufficiently soluble in DMF medium. Therefore, to keep consistency, solution studies of the complexes including catecholase activity (*vide infra*) were carried out in methanol/DMF (50:1 v/v) mixture. Electronic spectra of the complexes display broad absorption bands at 615 and 627 nm for complexes **1** and **2**, respectively. The positions of these bands are in agreement with the d-d transition of copper(II) ion found in similar complexes.^{52,53} Additionally, two distinct higher energy bands in the spectra of both the complexes appear at 353 and 462 nm for **1**, and 351 and 456 nm for **2**. Interestingly, the absorption spectrum of the Schiff base ligand alone shows only single $\pi \rightarrow \pi^*$ transition band at 339 nm which undoubtedly confirms that the bands at 462 nm for **1** and 456 nm for **2** are due the charge transfer (CT) transition. In order to understand origin of the charge transfer transition, a base titration of the ligand alone was conducted, and the resultant spectra are depicted in Fig. S1. This spectral titration shows that with addition of increasing

amount of base a new band is appeared at 430 nm, and as expected $\pi \rightarrow \pi^*$ transition band of the ligand at 339 nm is red-shifted about 6 nm due to deprotonation of the phenolic-OH. These results prompt us to conclude that the metal center does not participate in the charge transition in these complexes but it helps to deprotonate the phenolic-OH group thereby favoring the purely ligand-based charge transfer transition.

In order to confirm donor and acceptor parts of the CT transition, DFT study is carried out both for the ligand and a representative complex **2**. The calculated absorption peak at 350 nm is overlapped with another band at 387 nm for the ligand (Fig. S2). The oscillator strengths of these transitions are 0.438 and 0.139, respectively. The calculation of orbital contribution for these absorptions shows that 387 nm peak is due to HOMO to LUMO transition, while peak at 350 nm arises from HOMO-1 to LUMO (major) and HOMO-2 to LUMO (minor) transitions. The orbital contribution from groups in the ground state of the ligand shows that HOMO (-5.67 eV) is composed of 88% phenol moiety and 12% quinoline moiety, whereas HOMO-1 (-5.99 eV) is composed of 35% phenol moiety and 65% quinoline moiety, and HOMO-2(-6.77 eV) is composed of 51% phenol and 49% quinoline moiety. The experimental absorption peak observed at 339 nm is in very good agreement with the calculated peak. The orbital contributions also suggest that these two calculated absorption bands are inter ligand charge transfer (ILCT) character. The TDDFT calculation of the complex shows two bands at 487 and 372 nm in which oscillator strengths are 0.08 and 0.368, respectively (Fig. 1). The 487 nm peak can be assigned to the HOMO \rightarrow LUMO transition and the peak at 372 nm can be attributed to HOMO-1 \rightarrow LUMO and HOMO-1 \rightarrow LUMO+2. The orbital contribution also indicates that these transitions are ILCT character, and these transitions occur from phenol moiety as a donor to quinoline moiety as an acceptor.

Description of crystal structures of **1** and **2**

Complex **1** crystallizes in the monoclinic $P2_1/c$ space group, where the asymmetric unit corresponds to half of the molecule. The perspective view of **1** along with atom numbering scheme at metal coordination sphere is depicted in Fig. 2, while important bond distances and angles are given in Table 2. This centrosymmetric complex is formed by a bis($\mu_{1,1}$ -N₃)-bridged copper(II) dimer in which each of the copper(II) center is five-coordinate being bonded to three donor atoms from one mono-negative Schiff base ligand together with two nitrogen atoms (N3 and N3a) from two bridging azide groups. The coordination geometry of copper(II) ion can be best described as the ideal square pyramid as indicated by the Addison parameter (τ) of 0.052. Four atoms in the equatorial plane consist of three donor atoms from the tridentate ligand together with a nitrogen atom from a bridging azide with bond lengths of Cu1–O1 1.900(3) Å, Cu1–N1 1.993(4) Å, Cu1–N2 1.964(4) Å for tridentate ligand L and Cu1–N3 1.987(4) Å for azide ion. A second nitrogen atom (N3a) from centrosymmetrically related bridging azide coordinates an apical position at a rather long distance [2.505(4) Å], furnishing an elongated square-pyramidal geometry for each copper(II) center which is consistent with d^9 electronic configuration. The basal-apical bridging ultimately leads to an asymmetric $\mu_{1,1}$ bridging mode of azide ions in **1**. The bridging Cu1–N3–Cu1a angle is 89.7(1)° with metal–metal separation of 3.389(1) Å. The bridging N₃[−] anions are quasi-linear with N–N–N angles of 176.6(5)°. All the bond lengths and angles are within the range of those found in similar end-on azido-bridged copper(II) complexes of tridentate Schiff bases.^{54,55} Molecular packing of **1** is primarily stabilized by the π – π staking interactions between the adjacent quinoline rings as shown in Fig. 3.

Complex **2** crystallizes in the triclinic $P\bar{1}$ space group such that the asymmetric unit

contains two crystallographically independent molecules. A representative molecular structure along with selected atom numbering scheme is depicted in Fig. 4. X-ray crystallography reveals that copper(II) ion is four coordinate in square-planar environment being bonded with three donor atoms from mono-negative tridentate Schiff base ligand and a nitrogen atom from cyanate group. Further, average displacement of the metal centers from the respective N_3O least-square planes is found to be 0.026 Å, which indicates that coordination environment of the copper(II) ions in **2** is merely square-planar. Cu–N bond lengths vary in the range 1.924(2) to 2.012(2) Å, while Cu–O bond distances [1.891(2) and 1.915(2) Å] are close for two crystallographically independent molecules.^{54,55} The mono-anionic tridentate L ligand being planar the entire structure of complex **2** is also nearly planar although the cyanate group is coordinated to central Cu atom by the bent fashion at an angle C–N–Cu of 138.5(3)/148.0(3)°. This planarity helps to stabilize crystal packing by the strong π – π interactions between the adjacent molecules as depicted in Fig. 5.

From the crystal structures of complexes **1** and **2**, it is clear that in both the cases mono-negative Schiff base ligand binds the metal center in the planar arrangement which is consistent with the electronic structure of the ligand. But the diverse structural patterns in these complexes mainly arises from the mode of coordination of pseudohalides ligands. Azide being stronger bridging ligand bridges two metal centers in an end-on fashion, resulting as a formation of a dinuclear copper(II) complex **1**, while its congener cyanate ion only acts as a terminal ligand in **2**.

Catecholase activity

Catecholase activity is usually studied with 3,5-di-*tert*-butylcatechol (3,5-DTBC₂) as a model substrate because of its low redox potential that facilitates ease of oxidation of 3,5-DTBC₂ to its corresponding quinone, 3,5-di-*tert*-butylquinone (3,5-DTBQ), later of

which has a characteristic transition at about 400 nm. In order to check ability of the complexes to behave as catalysts for the catecholase activity, 2.0×10^{-5} M solutions of the complexes were treated with 200-fold concentrated solution of 3,5-DTBCH₂, and the spectra were recorded up to 2 h in dioxygen saturated methanol/DMF (50:1 v/v) at 25 °C. The time dependent spectral changes for a period of 2 h after the addition of 3,5-DTBCH₂ are shown in Fig. S3 (in ESI) & Fig. 6 for **1** and **2**, respectively. The spectral scan reveals the development of a strong absorption band at ca. 400 nm characteristic of quinone chromophore for **2**, while significant spectral growth was not observed for **1** in an identical condition. These spectral behaviors prompt us to conclude that complex **2** is reactive towards the catecholase activity, while complex **1** is almost inactive. It is worthy to note that after addition of substrate 3,5-DTBCH₂ to the solutions of the catalysts CT bands of the complexes did not disappear although progressive increase of quinone band along with the CT bands especially for **2** is observed. This observation suggests that destruction of the complex in terms of loss of coordinated Schiff base ligand in the presence of excess substrate is not happened, which not only proves the much stronger chelating ability of ligand L than that of the substrate but also rules out the possibility of any decomposition of active catalyst in terms of loss of coordinated ligands during the catalytic cycle.

Kinetic studies were performed to understand the extent of the catalytic efficiency of complex **2** as it exhibits reasonably good catecholase activity. For this purpose, 2×10^{-5} M solutions of the complex were treated with at least 10-fold concentrated substrate solution to maintain the pseudo-first-order condition. For a particular complex-substrate mixture, time scan at the maximum of quinone band was carried out for a period of 20 min, and initial rate was determined by linear regression from slope of the absorbance versus time. The initial rate of the reactions verses concentration of the substrate data show that rate is first order at the region of low concentrations of 3,5-DTBCH₂ but zero order at the higher concentrations

(Fig. 7). This observation suggests that quinone formation proceeds through a relatively stable intermediate, a complex-substrate adduct, followed by redox decomposition of the intermediate at the rate determining step. This type of saturation rate dependency on the concentration of the substrate may be explained by considering the Michaelis-Menten model, originally developed for the enzyme kinetics, which on linearization gives double reciprocal Lineweaver-Burk plot to analyze values of the parameters V_{\max} , K_M , and K_{cat} . The observed and simulated initial rates versus substrate concentration plot and the Lineweaver–Burk plot for complex **2** are shown in Fig. 7. Analysis of the experimental data yielded Michaelis binding constant (K_M) value of $2.27 \times 10^{-3} \text{ M}^{-1}$ and V_{\max} value of $1.31 \times 10^{-7} \text{ M}^{-1}$. The turnover number (K_{cat}) value is obtained by dividing the V_{\max} by the concentration of the catalyst, and is found to be 23.58 h^{-1} . Moreover, for a particular substrate concentration, varying the complex concentration, a linear relationship for the initial rates was obtained, which shows a first-order dependency on the catalyst concentration (Fig. S4).

Electrospray ionization mass spectral study

As compound **2** shows only catecholase activity, the electrospray ionization mass spectrum (ESI-MS positive) of methanol/DMF solution of compound **2** was recorded and is shown in Fig. S5. Compound **2** exhibits five assignable peaks at $m/z = 339.83$, 404.78 , 420.74 , 721.63 and 786.55 with line-to-line separation of 1.0. The peaks at $m/z = 339.83$, 404.78 and 420.74 arise from the monomeric entity of the complex and are assigned to $[\text{Cu}^{\text{II}}\text{L}]^+$, $[\text{NaCu}^{\text{II}}\text{L}(\text{NCO})]^+$ and $[\text{KCu}^{\text{II}}\text{L}(\text{NCO})]^+$, respectively, while low intense peaks at $m/z = 721.63$ and 786.55 appear due to the dimeric aggregate of the complex and these can be assigned to $[\text{Cu}^{\text{II}}_2\text{L}_2(\text{NCO})]^+$ and $[\text{NaCu}^{\text{II}}_2\text{L}_2(\text{NCO})_2]^+$, respectively. All these

monopositive species are well matched with the simulated isotropic distribution pattern as shown in Fig. S5.

In order to get further insight into the nature of possible complex–substrate intermediates, ESI-MS positive spectrum of a mixture of complex **2** and 3,5-DTBCH₂ in 1 : 50 molar ratio was recorded after 5 minutes of mixing in methanol/DMF. The observed and simulated patterns are presented in Fig. 8. As can be seen from the figure, the most abundant species found at m/z 340.05 in the mass spectrum corresponds to the original compound **2** and it can be assigned to $[\text{Cu}^{\text{II}}\text{L}]^+$. The peak at 243.16 is well assignable to the quinone-sodium aggregate $[\text{3,5-DTBQ-Na}]^+$. The remaining peak at $m/z = 584.19$ including two minor peaks at $m/z = 616.13$ and 923.21 are quite interesting because the peak position, line-to-line separation, and matching of the isotopic distributions of the observed and the simulated patterns (Fig. 8) clearly indicate that these peaks arise from complex-substrate aggregates. More specifically these peaks at $m/z = 584.19$, 616.13 and 923.21 can be assigned to $[\text{NaCu}^{\text{II}}\text{L}(3,5\text{-DTBCH})]^+$, $[\text{NaCuL}(\text{O}_2)(3,5\text{-DTBCH})]^+$ and $[\text{NaCu}_2^{\text{II}}\text{L}_2(3,5\text{-DTBCH})]^+$, respectively. Although mass spectroscopy does not necessarily mirror the species present in the solution state yet it provides significant information based on that one could get a mechanistic inference of a catalytic process.

Plausible mechanism and DFT studies

At this juncture, it is to be mentioned that the catechol oxidase activity depends on several factors namely Cu...Cu distance, geometry around the metal center, nature of the exogenous ligand, and flexibility of the primary ligand. The metal-metal separation (3.398 Å) in complex **1** lies in the range where catecholase activity of several systems is found to be very efficient.¹⁴⁻²⁷ Complex **1** is EPR silent at 77K which ensures that the dimer preserves its integrity in acetonitrile/DMF solution. Thus the lack of activity of complex **1**

towards the catecholase activity may be due to the fact that the doubly bridging dicopper(II) system is substitutionally inert for incoming substrate.^{56,57} Inactivity of the complex further suggests that although one of the apical position is available but copper(II) center is reluctant to increase its coordination number up to six. It is also interesting to note that as the geometry of the copper(II) center is a trigonal pyramidal in the crystal structure of met form of the enzyme, most of the efficient models reported in the literature are found to be non-planar structures.^{14-17, 19-27} Only limited numbers of square planar complexes are known which show catecholase activity.¹⁸ In the present case, the moderately strong activity as suggested by the turnover number for mononuclear complex **2** would definitely be a significant contribution towards the modeling of the catechol oxidase. Either of the vacant apical positions or substitutionally labile cyanate ion favors the binding of the substrate with copper(II) center thereby leading to exhibit moderately strong catecholase activity.

The EPR spectrum of complex **2** is typical for mononuclear copper(II) complexes (Fig. S6), but on addition of 3,5-DTBC₂, the characteristic signal for copper(II) ion was disappeared which suggests that copper(II) center is reduced to copper(I) state in the catalytic cycle. It is now well known that catechol oxidation by dicopper(II) complexes takes place by the transfer of couple of electrons from substrate to copper(II) centers. But mononuclear copper(II) complex in the present case could only act as single electron oxidant, and thus it could be possible that 3,5-DTBC₂ bridges two neighboring mononuclear copper(II) centers followed by the electron transfer to copper(II) centers in the rate determining step. Although a species of formula $[\text{NaCu}_2^{\text{II}}\text{L}_2(3,5\text{-DTBC})]^+$ is identified in the mass spectroscopy, unimolecular rate of the reaction with respect to complex **2** clearly precludes the possibility of involvement of two copper(II) centers in the main catalytic cycle. The possibility of involvement of phenolate radical as a second oxidant can also be neglected as the electrochemical study suggests that the oxidation of phenolate ion is

quite difficult. Therefore, the dioxygen-bound copper species could probably be the active catalyst for the oxidation of 3,5-DTBCH₂. Both the substrate and dioxygen bound species, Na[CuL(O₂)(3,5-DTBCH)]⁺, identified in the mass spectroscopy supports the above fact.

We are at the stage to tempt a plausible pathway in which at the first stage active catalyst (**B**) is generated by the reaction of 3,5-DTBCH₂ with two equivalents of complex **2** (Scheme 2). That catecholate bound copper(I) complex (**B**) is supposed to act as the active catalyst to generate the superoxide intermediate (**C**) by the reaction with aerial oxygen in which copper(I) center in **B** undergoes an oxidation to a copper(II) center in **C** (Scheme 3). In the catalytic cycle, next step involves the intramolecular proton transfer process from oxygen atom of catechol moiety to the superoxide oxygen atom in intermediate **C** via a transition state **D** to produce a peroxo-intermediate **E**. Finally, the last step involves the binding of another molecule of substrate, 3,5-DTBCH₂, to the copper center in **E** regenerating the starting **B** species with concomitant release of the desired 3,5-DTBQ.

The proposed mechanistic pathway for the catechol oxidation by molecular dioxygen in the presence of complex **2** as a catalyst is further supported by the density functional theory (DFT) study. As expected theoretical calculations show that the Mulliken charge on Cu center in **C** is changed to 0.490 from 0.315 in **B**, and the bond length of molecular oxygen (1.21Å) is changed to superoxide (1.31 Å) in **C** (Table S1). The O–O bond in the transition state **D** has been elongated to 1.34 Å compared with 1.31 Å in **C**. The Mulliken charge of Cu in **D** transition state is slightly increased to 0.490 in comparison to 0.452 in **C**. Whereas the Mulliken charge on superoxide-O atoms (–0.253 and –0.251) in intermediate **C** changed to –0.302 and –0.341 in **D** transition state, respectively. This change of charge density suggests proton transfer occurs from catecholate-O to the superoxide-O atom. As expected the elongated O–O peroxide bond distance of 1.42Å is observed in peroxide intermediate state **E**. Consequently the semiquinone character of the catechol moiety is

observed in the intermediate state **E** having shorter C–O bond lengths (1.26 and 1.28 Å) compared to catecholate functionality (1.35 and 1.31 Å) in superoxo intermediate **C**.^{58,59} The proton transfer is also corroborated by shifting of the Mulliken charge of peroxide (in intermediate **E**) oxygen atoms –0.525 and –0.561 compared to that of the superoxide oxygen atoms –0.253 and –0.251 in intermediate **C**. Therefore both the experimental facts and theoretical study (Table S1 and Fig S7) agree well with the proposed mechanistic pathway for the catalytic oxidation of 3,5-DTBCH₂ by molecular dioxygen in the presence of complex **2** as a catalyst.

Conclusion

Two new di- and mono-nuclear copper(II) complexes have been synthesized from a planar tridentate ligand 2-methoxy-6-(8-iminoquinolinylmethyl)phenol (HL) together with pseudohalides as coligands. Structural characterizations reveal that complex **1** is a centrosymmetric bis(azide)-bridged dimer in which copper(II) centers reside in the square pyramidal environment while it is square planar in **2**. From the crystal structure it is clear that pseudohalide coligands have diverse impact on the nuclearity of those complexes - azide ions bind the metal centers in an end-on asymmetric bridging fashion in **1**, whereas cyanate ion simply acts as a monodentate terminal ligand in **2**. Although the crystal structure of the native met form of catechol oxidase suggested a dicopper(II) system, but in the present investigation dinuclear compound **1** is found to be almost inactive. On the other hand, mononuclear compound **2** exhibits significant catecholase activity which is probably due to the presence of labile cyanate ion together with unsaturated coordination number that favors binding of substrate to the metal center. The ESI-MS positive spectrum of the mixture of complex **2** and 3,5-DTBCH₂ shows a peak corresponding to Na[CuL(O₂)(3,5-DTBCH)]⁺, suggesting simultaneous coordination of the substrate and

molecular dioxygen to the metal center in the catalytic cycle. Interestingly, complex **2** not only represents the mononuclear class of copper(II) compounds that rarely investigated for the catecholase mimicking activity but also the first example of a mononuclear square planar complex exhibiting catechol oxidase activity.

Acknowledgements

M. S. thanks the University Grant Commission, India for a Fellowship. A. S. gratefully acknowledges the financial support of this work by the DST, India (Sanction No. SB/EMEQ-159/2013 date 10/10/2013). A. P. also gratefully acknowledges the financial support of this work by the University Grant Commission, India (Sanction No. PSW-173/11-12). The ESI-MS spectra facility was availed from the Indian Association for the Cultivation of Science, India. Crystallography was performed at the DST-FIST, India, funded single crystal diffractometer facility at the Department of Chemistry, Jadavpur University, India.

† Electronic supplementary information (ESI) available: The electronic supplementary information file contains Figs. S1–S6 and Table S1. CCDC 956080 and 956081 contain the supplementary crystallographic data for **1** and **2**, respectively. For ESI and crystallographic data in CIF or other electronic format see DOI: To be filled by the publisher.

References

- 1 E. I. Solomon, R. Sarangi, J. S. Woertink, A. J. Augustine, J. Yoon and S. Ghosh, *Acc. Chem. Res.*, 2007, **40**, 581.

- 2 P. C. A. Bruijninx, G. van Koten and R. J. M. Klein Gebbink, *Chem. Soc. Rev.*, 2008, **37**, 2716.
- 3 S. Friedle, E. Reisner and S. J. Lippard, *Chem. Soc. Rev.*, 2010, **39**, 2768.
- 4 R. Hage and A. Lienke, *Angew. Chem.*, 2006, **118**, 212.
- 5 N. Duran and E. Esposito, *Appl. Catal. B*, 2000, **28**, 83.
- 6 M. Costas, M.P. Mehn, M.P. Jensen and L. Que Jr., *Chem. Rev.*, 2004, **104**, 939.
- 7 L. Que and W. B. Tolman, *Nature*, 2008, **455**, 333.
- 8 E.B. Meunier, *Biomimetic Oxidations Catalyzed by Transition Metal Complexes*, Imperial College Press, London, 2000.
- 9 T. Klabunde, C. Eicken, J. C. Sacchettini and B. Krebs, *Nat. Struct. Biol.*, 1998, **5**, 1084.
- 10 I. A. Koval, P. Gamez, C. Belle, K. Selmeczi and J. Reedijk, *Chem. Soc. Rev.*, 2006, **35**, 814.
- 11 K. Selmeczi, M. Reglier, M. Giorgi and G. Speier, *Coord. Chem. Rev.*, 2003, **245**, 191.
- 12 R. Than, A. A. Feldmann and B. Krebs, *Coord. Chem. Rev.*, 1999, **182**, 211.
- 13 B. J. Dervall, *Nature*, 1961, **189**, 311.
- 14 N. A. Rey, A. Neves, A. J. C. T. Bortoluzzi, Pich and H. Terenzi, *Inorg. Chem.*, 2007, **46**, 348.
- 15 C. Belle, C. Beguin, I. Gautier-Luneau, S. Hamman, C. Philouze, J. L. Pierre, F. Thomas and S. Torelli, *Inorg. Chem.*, 2002, **41**, 479.
- 16 J. Anekwea, A. Hammerschmidta, A. Rompelb and B. Krebs, *Z. Anorg. Allg. Chem.*, 2006, **632**, 1057.
- 17 J. Ackermann, F. Meyer, E. Kaifer and H. Pritzkow, *Chem. Eur. J.* 2002, **8**, 247.
- 18 J. Mukherjee and R. Mukherjee, *Inorg. Chim. Acta*, 2002, **337**, 429.

- 19 M. Merkel, N. Mçller, M. Piacenza, S. Grimme, A. Rompel and B. Krebs, *Chem. Eur. J.*, 2005, **11**, 1201.
- 20 C. Fernandes, A. Neves, J. Bortoluzzi, A. S. Mangrich, E. Rentschler, B. Szpoganicz and E. Schwingel, *Inorg. Chim. Acta*, 2001, **320**, 12.
- 21 A. Neves, L. M. Rossi, A. J. Bortoluzzi, A. S. Mangrich, W. Haase and R. Werner, *J. Braz. Chem. Soc.*, 2001, **12**, 747.
- 22 P. K. Nanda, V. Bertolasi, G. Aromí and D. Ray, *Polyhedron*, 2009, **27**, 987.
- 23 R. Gupta, S. Mukherjee and R. Mukherjee, *Polyhedron*, 2000, **19**, 1429.
- 24 A. Majumder, S. Goswami, S. R. Batten, M. S. El Fallah, J. Ribas and S. Mitra, *Inorg. Chim. Acta*, 2006, **359**, 2375.
- 25 C.-H. Kao, H.-H. Wei, Y.-H. Liu, G.-H. Lee, Y. Wang and C.-J. Lee, *J. Inorg. Biochem.*, 2001, **84**, 171.
- 26 M. Thirumavalavan, P. Akilan, M. Kandaswamy, G. Chinnakali, G. Senthil Kumar and H. K. Fun, *Inorg. Chem.*, 2003, **42**, 3308.
- 27 S. J. Smith, C. J. Noble, R. C. Palmer, G. R. Hanson, G. Schenk, L. R. Gahan and M. Riley, *J. Biol. Inorg. Chem.*, 2008, **13**, 499.
- 28 E. I. Solomon, U. M. Sundaram and T. E. Machonkin, *Chem. Rev.*, 1996, **96**, 2563.
- 29 N. Kitajima and Y. Moro-oka, *Chem. Rev.*, 1994, **94**, 737.
- 30 C. Eicken, B. Krebs and J. C. Sacchettini, *Curr. Opin. Struct. Biol.*, 1999, **9**, 677.
- 31 M. K. Panda, M. M. Shaikh, R. J. Butcher and P. Ghosh, *Inorg. Chim. Acta*, 2011, **372**, 145.
- 32 G. Grigoropoulou, K.C. Christoforidis, M. Louloudi and Y. Deligiannakis, *Langmuir*, 2007, **23**, 10407.
- 33 G. Speier, *J. Mol. Catal.*, 1986, **37**, 259.

- 34 Z.-F. Chen, Z.-R. Liao, D.-F. Li, W.-K. Li and X.-G. Meng, *J. Inorg. Biochem.*, 2004, **98**, 1315.
- 35 Á. Kupán, J. Kaizer, G. Speier, M. Giorgi, M. Réglíer and F. Pollreisz, *J. Inorg. Biochem.*, 2009, **103**, 389.
- 36 S. Majumder, S. Sarkar, S. Sasmal, E. C. Sañudo and S. Mohanta, *Inorg. Chem.*, 2011, **50**, 7540.
- 37 A. Panja, M. Shyamal, A. Saha and T. K. Mandal, *Dalton Trans.*, 2014, **43**, 5443.
- 38 A. Panja, *Dalton Trans.*, 2014, **43**, 7760.
- 39 A. Panja and P. Guionneau, *Dalton Trans.*, 2013, **42**, 5068.
- 40 A. Panja, *RSC Adv.*, 2014, **4**, 37085.
- 41 A. Panja, S. Goswami, N. Shaikh, P. Roy, M. Manassero, R. J. Butcher and P. Banerjee, *Polyhedron*, 2005, **24**, 2921.
- 42 S. Nayak, P. Gamez, B. Kozlevčar, A. Pevec, O. Roubeau, S. Dehnen and J. Reedijk, *Polyhedron*, 2010, **29**, 2291.
- 43 G. M. Sheldrick, SAINT, Version 6.02, SADABS, Version 2.03, Bruker AXS Inc., Madison, Wisconsin, 2002.
- 44 G.M. Sheldrick, SHELXL-97, Crystal Structure Refinement Program, University of Gottingen, 1997.
- 45 M. J. Frisch, G. W. Trucks, H. B. Schlegel, G. E. Scuseria, M. A. Robb, J. R. Cheeseman, G. Scalmani, V. Barone, B. Mennucci, G. A. Petersson, H. Nakatsuji, M. Caricato, X. Li, H. P. Hratchian, A. F. Izmaylov, J. Bloino, G. Zheng, J. L. Sonnenberg, M. Hada, M. Ehara, K. Toyota, R. Fukuda, J. Hasegawa, M. Ishida, T. Nakajima, Y. Honda, O. Kitao, H. Nakai, T. Vreven, J. A. Montgomery, Jr., J. E. Peralta, F. Ogliaro, M. Bearpark, J. J. Heyd, E. Brothers, K. N. Kudin, V. N. Staroverov, R. Kobayashi, J. Normand, K. Raghavachari, A. Rendell, J. C. Burant, S.

- S. Iyengar, J. Tomasi, M. Cossi, N. Rega, J. M. Millam, M. Klene, J. E. Knox, J. B. Cross, V. Bakken, C. Adamo, J. Jaramillo, R. Gomperts, R. E. Stratmann, O. Yazyev, A. J. Austin, R. Cammi, C. Pomelli, J. W. Ochterski, R. L. Martin, K. Morokuma, V. G. Zakrzewski, G. A. Voth, P. Salvador, J. J. Dannenberg, S. Dapprich, A. D. Daniels, Ö. Farkas, J. B. Foresman, J. V. Ortiz, J. Cioslowski and D. J. Fox, Gaussian 09, Revision A.02, Gaussian, Inc., Wallingford CT, 2009.
- 46 P. Manikandan, R. Muthukumaran, K.R. Justin Thomas, B. Varghese, G.V.R. Chandramouli and P.T. Manoharan, *Inorg. Chem.*, 2001, **40**, 2378.
- 47 S. Koner, S. Saha, K.-I. Okamoto and J.-P. Tuchagues, *Inorg. Chem.*, 2003, **42**, 4668.
- 48 S. Koner, S. Saha, T. Mallah and K.I. Okamoto, *Inorg. Chem.*, 2004, **43**, 840.
- 49 A. Escuer, M. F. Bardía, S. S. Massoud, F.A. Mautner, E. Peñalba, X. Solans and R. Vicente, *New. J. Chem.*, 2004, **28**, 681.
- 50 J. D. Woodward, R.V. Backov, K.A. Abboud, D. Dai, H.-J. Koo, M.-H. Whangbo, M. W. Meisel and D. R. Talham, *Inorg. Chem.*, 2005, **44**, 638.
- 51 M. Zbiri, S. Saha, C. Adhikary, S.C. Daul and S. Koner, *Inorg. Chim. Acta*, 2006, **359**, 1193.
- 52 M. Dolai, T. Mistri, A. Panja and M. Ali, *Inorg. Chim. Acta*, 2013, **399**, 95.
- 53 C.-T. Yang, M. Vetrichelvan, X. Yang, B. Moubaraki, K. S. Murray and J. J. Vittal, *Dalton Trans.*, 2004, 113.
- 54 M. S. Ray, A. Ghosh, S. Chaudhuri, M. G. B. Drew and J. Ribas, *Eur. J. Inorg. Chem.*, 2004, 3110.
- 55 S. Naiya, S. Biswas, M. G.B. Drew, C. J. Gómez-García and A. Ghosh, *Inorg. Chim. Acta*, 2011, **377**, 26–33.
- 56 A. Banerjee, R. Singh, E. Colacio and K. K. Rajak, *Eur. J. Inorg. Chem.*, 2009, 277.

- 57 S. Sarkar, S. Majumder, S. Sasmal, L. Carrella, E. Rentschler and S. Mohanta, *Polyhedron*, 2013, **50**, 270.
- 58 N. Shaikh, S. Goswami, A. Panja, X.-Y. Wang, S. Gao, R.J. Butchler and P. Banerjee, *Inorg. Chem.*, 2004, **43**, 5908.
- 59 A. Panja, *RSC Adv.*, 2013, **3**, 4954.

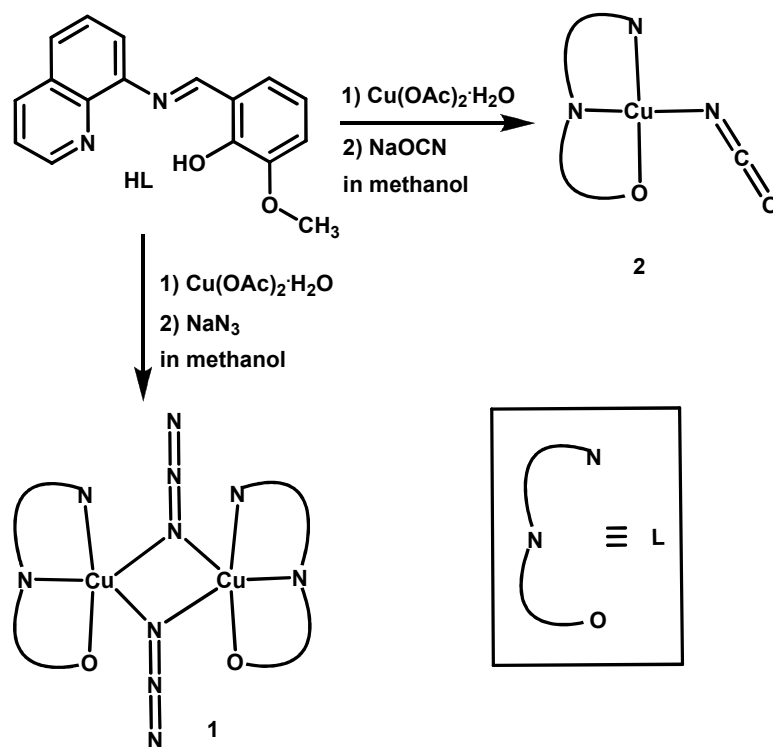
Table 1. Crystal data and structure refinement of **1** and **2**

Compound	1	2
Empirical formula	C ₃₄ H ₂₆ N ₁₀ O ₄ Cu ₂	C ₁₈ H ₁₃ N ₃ O ₃ Cu
Formula weight	765.73	382.85
Temperature (K)	298 (2)	298 (2)
Wavelength (Å)	0.71073	0.71073
Crystal system	Monoclinic	Triclinic
Space group	P2 ₁ /c	P $\bar{1}$
<i>a</i> (Å)	9.0785(6)	7.2980(2)
<i>b</i> (Å)	22.8156(16)	14.4856(5)
<i>c</i> (Å)	8.3584(5)	14.9016(5)
α (°)	90	85.634(2)
β (°)	115.520(4)	83.851(2)
γ (°)	90	78.042(2)
Volume (Å ³)	1562.37(18)	1529.93(8)
<i>Z</i>	2	4
<i>D</i> _{calc} (g cm ⁻³)	1.628	1.662
Absorption coefficient (mm ⁻¹)	1.420	1.451
<i>F</i> (000)	780	780
θ Range for data collection (°)	1.79–26.43	1.94–27.24
Reflections collected	23810	24661
Independent reflection / <i>R</i> _{int}	1573/0.1356	4653 / 0.0425
Data / restraints / parameters	3211/0/226	6762 / 0 / 453
Goodness-of-fit on <i>F</i> ²	0.962	1.020
Final <i>R</i> indices [<i>I</i> >2 σ (<i>I</i>)]	<i>R</i> 1 = 0.0547, w <i>R</i> 2 = 0.0988	<i>R</i> 1 = 0.0428, w <i>R</i> 2 = 0.0940
<i>R</i> indices (all data)	<i>R</i> 1 = 0.1424, w <i>R</i> 2 = 0.1231	<i>R</i> 1 = 0.0704, w <i>R</i> 2 = 0.1045
Largest diff. peak / hole (e Å ⁻³)	0.318/−0.356	0.472/ −0.311

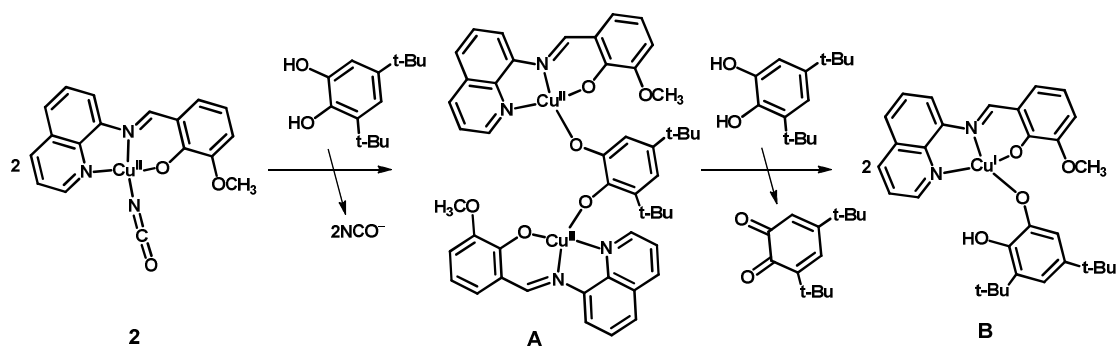
Table 2. Selected bond lengths (Å) and bond angles (°) for **1** and **2**

	1		2
Cu1–O1	1.900(3)	Cu1–O1	1.891(2)
Cu1–N1	1.993(4)	Cu1–N1	1.989(2)
Cu1–N2	1.964(4)	Cu1–N2	1.949(2)
Cu1–N3	1.987(4)	Cu1–N3	1.931(3)
Cu1–N3a	2.505(4)	Cu2–O4	1.915(2)
		Cu2–N4	2.012(2)
		Cu2–N5	1.954(2)
		Cu2–N6	1.924(2)
N2–Cu1–N1	81.96(17)	N2–Cu1–N1	82.51(9)
O1–Cu1–N2	92.75(16)	O1–Cu1–N2	92.75(16)
N2–Cu1–N3	172.94(15)	O1–Cu1–N1	169.82(14)
O1–Cu1–N1	169.82(14)	N2–Cu1–N3	172.94(15)
N5–N4–N3	176.6(5)	N5–Cu2–N4	82.12(9)
Cu1–N3–Cu1a	97.3(2)	O4–Cu2–N5	92.84(8)
		O4–Cu2–N4	174.87(8)
		N6–Cu2–N5	174.51(10)

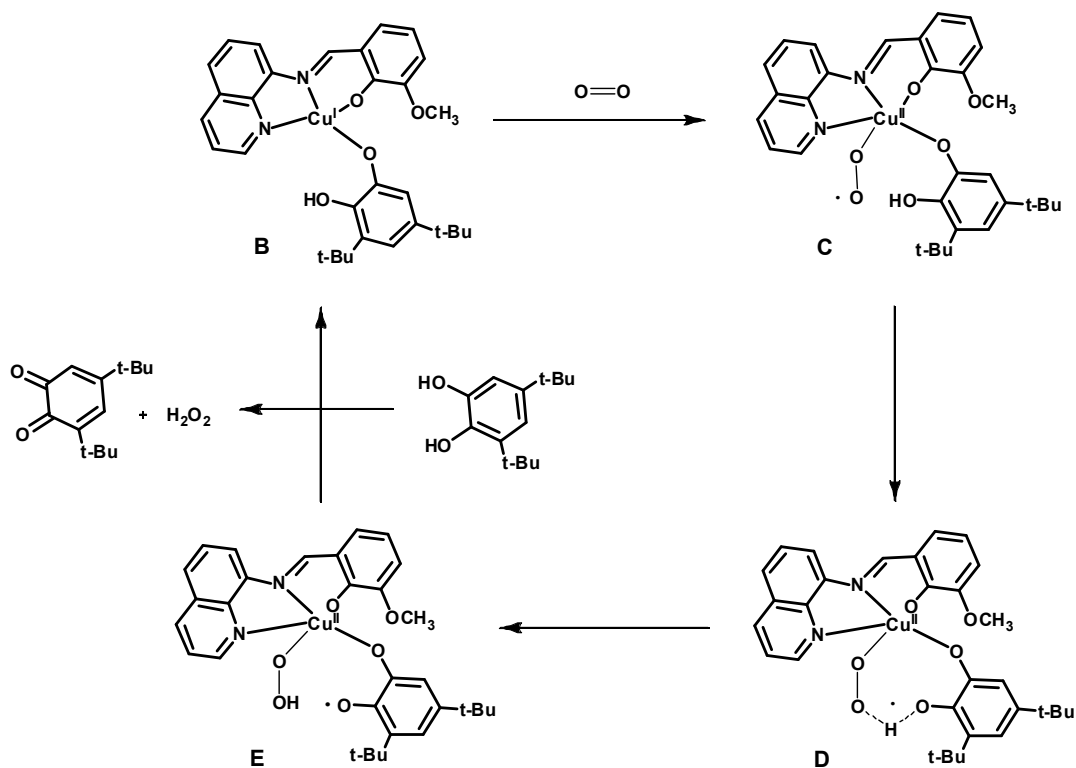
Symmetry code: a = 2 – x, –y, 1 –z.



Scheme 1. Route to the syntheses of complexes 1 and 2



Scheme 2. Probable pathway for the generation of the precatalyst



Scheme 3. Probable catalytic cycle for the oxidation of 3,5-DTBCH₂ by complex 2

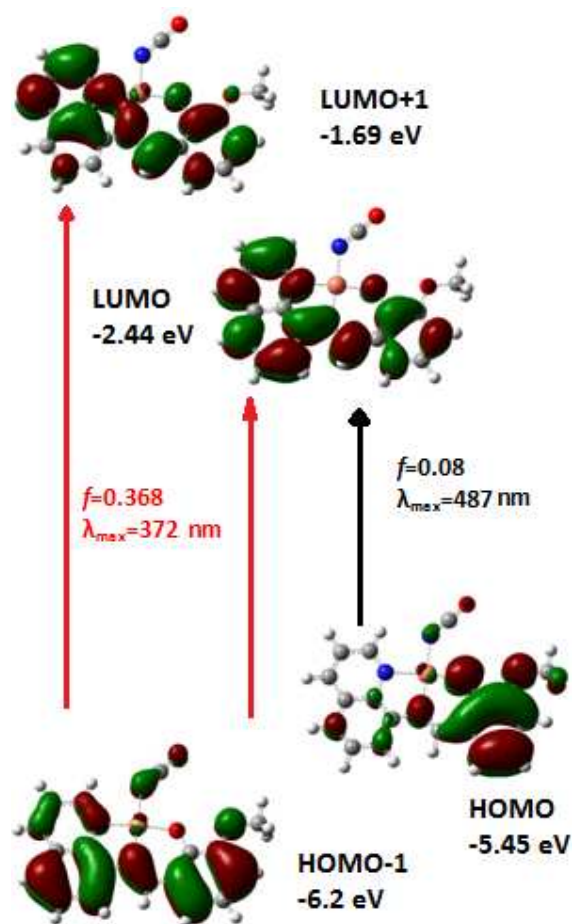


Fig. 1 Frontier molecular orbitals involved in UV-Vis absorption of complex 2.

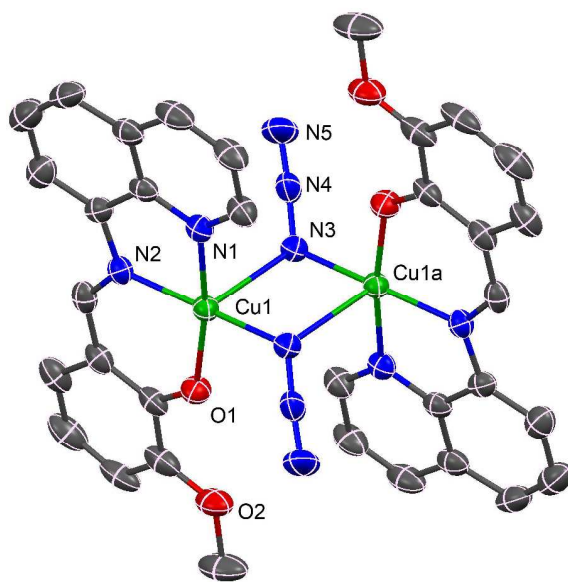


Fig. 2 Crystal structure of **1** showing the atom numbering scheme. Ellipsoids are drawn at 30% probability level. H atoms are omitted for clarity. Symmetry code: $a = 2 - x, -y, 1 - z$.

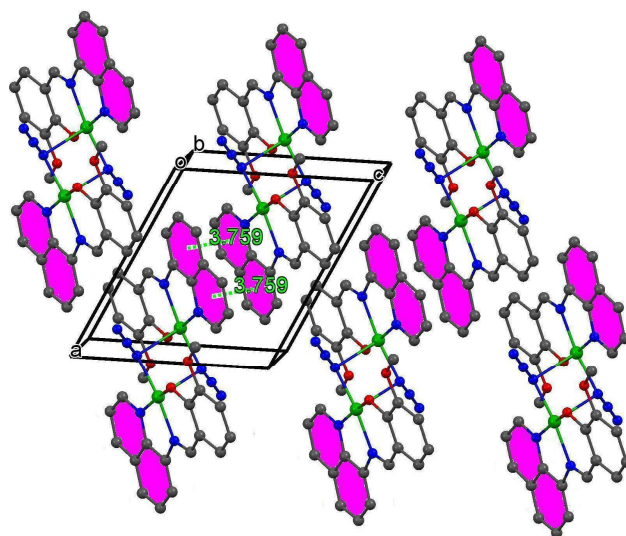


Fig. 3 Crystal packing of complex **1** showing π - π stacking interactions.

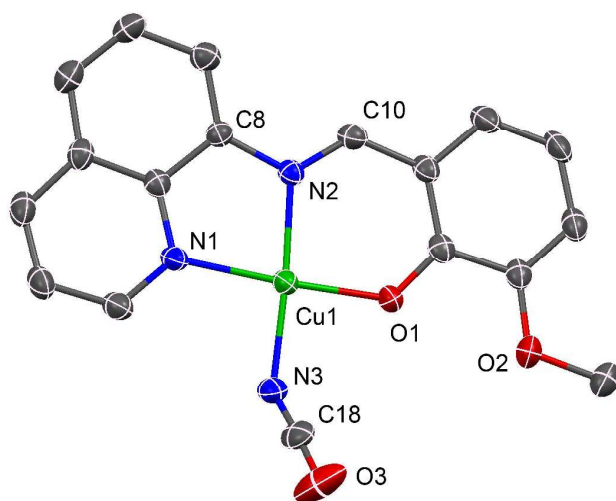


Fig. 4 A representative ORTEP-type plot of the structure of **2** with selected atom numbering scheme. Ellipsoids are drawn at 30% probability level and H atoms are omitted for clarity.

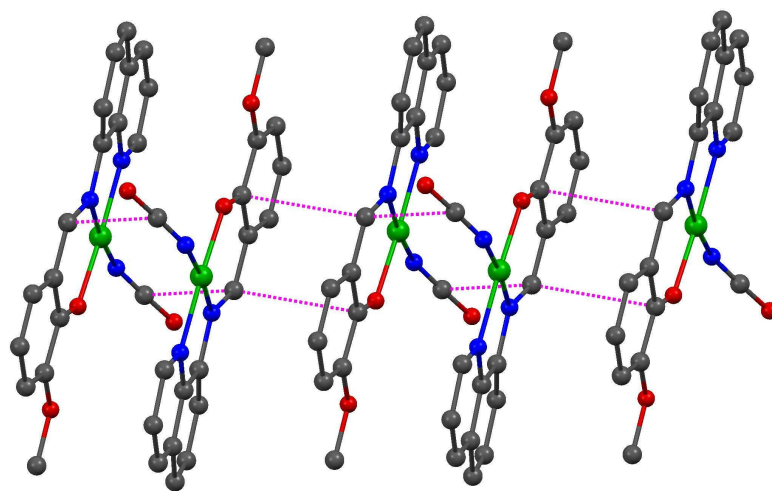


Fig. 5 A part of molecular packing of **2** showing different kinds of π - π interactions.

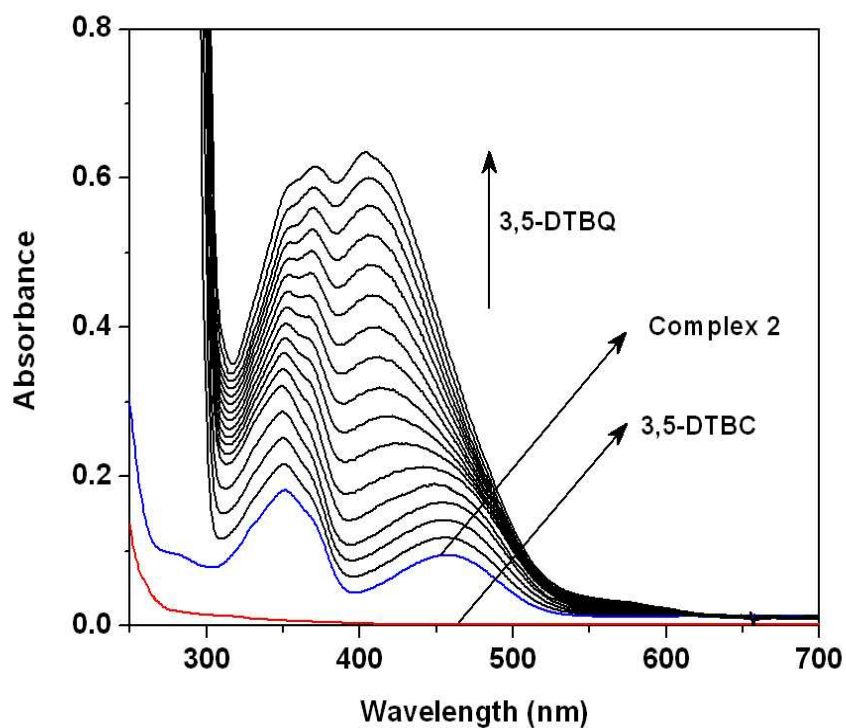


Fig. 6 UV-vis spectral profile showing the growth of quinine band at 405 nm after the addition of 200-fold 3,5-DTBCH₂ to a solution containing complex **2** (2×10^{-5} M) in dioxygen saturated MeOH/DMF (50:1) at 25 °C. The spectra were recorded for the period of 2h.

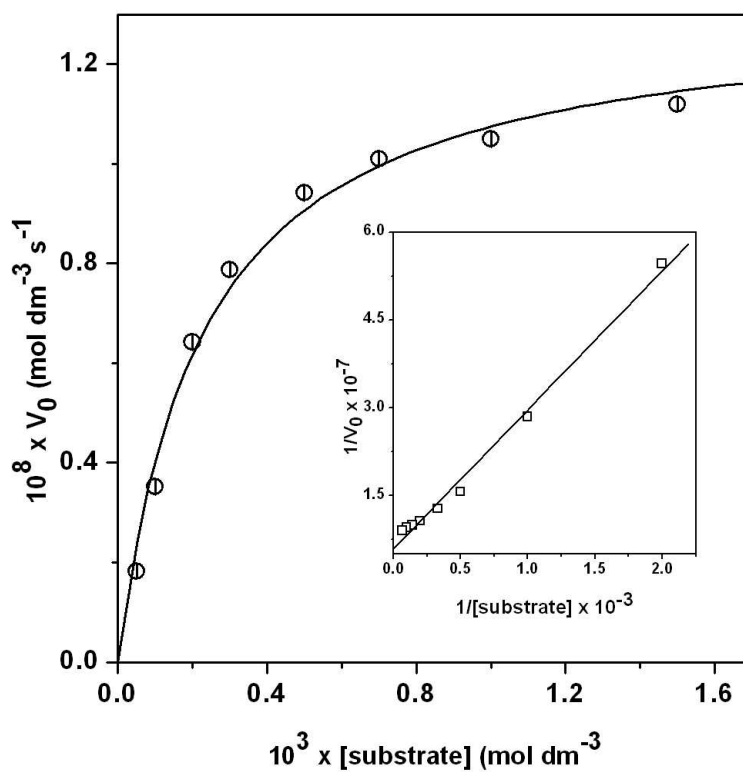


Fig. 7 Plot of the initial rates versus substrate concentration for the oxidation reaction catalyzed by complex **2** at a fixed concentration in dioxygen-saturated MeOH/DMF (50:1) at 25 °C. Inset shows Lineweaver–Burk plot. Symbols and solid lines represent the experimental and simulated profiles, respectively.

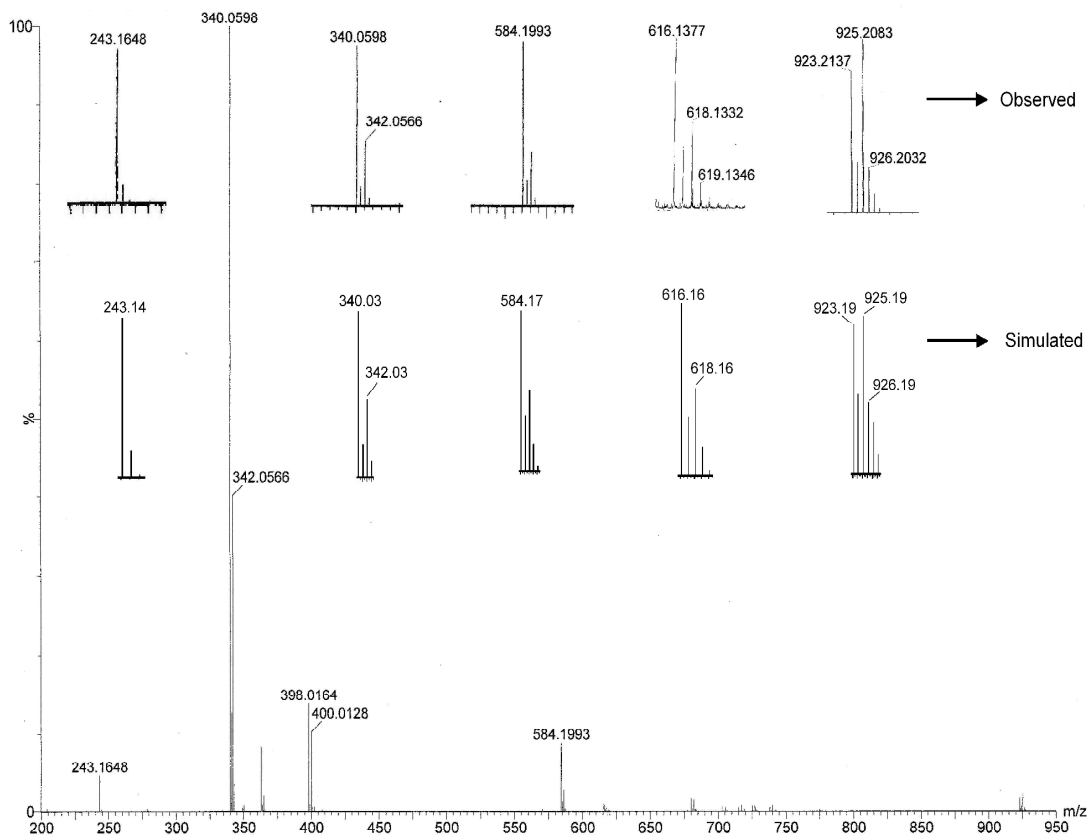


Fig. 8 Electrospray ionization mass spectrum (ESI-MS positive) of a 1:50 mixture of [CuL(NCO)] (2) and 3,5-DTBCH₂ in methanol/DMF, recorded after 5 minutes of mixing. Both the observed and simulated isotopic distribution patterns are shown.

Graphical Abstract

Influence of anionic coligands on the structural diversity and on the catecholase activity in mono- and di-nuclear copper(II) systems

Milan Shyamal, Tarun Kanti Mandal, Anangamohan Panja and Amrita Saha

Role of the exogenous pseudohalide coligands on the structural diversity and on the relative catecholase activity of the complexes have also been explored. The dicopper(II) complex is almost inactive while monomer shows moderately strong catecholase activity. The reported copper(II) complex is the first example of a mononuclear square planar complex exhibiting catechol oxidase activity.

